

# Pattern Synthesis via Complex-Coefficient Weight Vector Orthogonal Decomposition—Part II: Robust Sidelobe Synthesis

Xuejing Zhang, *Student Member, IEEE*, Zishu He, *Member, IEEE*, and Xuepan Zhang

**Abstract**—In this paper, the complex-coefficient weight vector orthogonal decomposition ( $C^2$ -WORD) algorithm proposed in Part I of this two paper series is extended to robust sidelobe control and synthesis with steering vector mismatch. Assuming that the steering vector uncertainty is norm-bounded, we obtain the worst-case upper and lower boundaries of array response. Then, we devise a robust  $C^2$ -WORD algorithm to control the response of a sidelobe point by precisely adjusting its upper-boundary response level as desired. To enhance the practicality of the proposed robust  $C^2$ -WORD algorithm, we also present detailed analyses on how to determine the upper norm boundary of steering vector uncertainty under various mismatch circumstances. By applying the robust  $C^2$ -WORD algorithm iteratively, a robust sidelobe synthesis approach is developed. In this approach, the upper-boundary response is adjusted in a point-by-point manner by successively updating the weight vector. Contrary to the existing approaches, the devised robust  $C^2$ -WORD algorithm has an analytical expression and can work starting from an arbitrarily-specified weight vector. Simulation results are presented to validate the effectiveness and good performance of the robust  $C^2$ -WORD algorithm.

**Index Terms**—Array pattern synthesis, robust sidelobe synthesis, robust sidelobe control, steering vector mismatch.

## I. INTRODUCTION

IN the companion paper [1], an array response control scheme named complex-coefficient weight vector orthogonal decomposition ( $C^2$ -WORD) was proposed and analyzed. In  $C^2$ -WORD, the given weight vector is orthogonally decomposed as two parts. We realize precise array response control of a given point by adjusting the combining coefficient (in complex domain) of the two orthogonal vectors. The  $C^2$ -WORD scheme can work from an arbitrarily-specified weight vector. Moreover, it brings less pattern variations at the uncontrolled points. As presented in [1], one can synthesize desirable patterns by successively choosing the angle to be controlled and applying  $C^2$ -WORD approach.

In  $C^2$ -WORD, the array steering vectors are assumed to be known exactly. Under practical circumstances, however, the actual steering vectors may be different from the assumed (or ideal) ones. The steering vector uncertainty can be caused by various factors such as, channel gain-phase mismatch, element position mismatch and mutual coupling effect. The existence

of steering vector uncertainties may lead to performance degradation for  $C^2$ -WORD algorithm on array response control and pattern synthesis.

During the past several decades, quite a number of robust algorithms have been developed to control array response or synthesize desirable beampatterns with steering vector uncertainties. For example, authors of [2] proposed a powerful robust approach to synthesizing array patterns with low sidelobes in the presence of unknown array manifold perturbations. This approach optimizes the worst-case performance of sidelobe response by formulating the robust pattern synthesis problem as a convex programming (CP) form. Nevertheless, this method can only synthesize uniform sidelobes and may not work well if the sidelobe shape is arbitrarily-specified. A novel robust beampattern synthesis method is proposed in [3], where the mutual coupling effect is considered and two optimization methods are provided. Nevertheless, the mutual coupling matrix has to be pre-calculated in this approach before the synthesis process. Efficient robust broadband antenna array pattern synthesis techniques in the presence of array imperfections have been presented in [4], where nine different optimization criteria are provided with each one having particular advantages and disadvantages for certain applications. In contrast to the above deterministic pattern synthesis methods, there are also some excellent works considering robust adaptive beamforming with steering vector uncertainties, see [5]–[9]. In this case, it is usually required to shape satisfactory beampatterns and reject the undesirable interferences. In addition, it should be pointed out that our discussions are different from the pattern tolerance analyses in [10]–[14], where the weight vector (but not the steering vector) suffers from perturbation.

In general, the existing methods cannot flexibly control the array response starting from an arbitrarily-specified weight vector. As a result, the weight vector has to be completely redesigned even if only a slight change of the desired pattern is needed. This motivates us to develop a new array response control algorithm with steering vector perturbations. Toward this end, in this paper we modify the  $C^2$ -WORD algorithm in [1] and develop a new scheme named robust  $C^2$ -WORD. Starting from an any given weight vector, the proposed robust  $C^2$ -WORD algorithm can control the array response level of a single sidelobe point when array suffers from unknown steering vector mismatches. More specifically, assuming that the steering vector perturbation is norm-bounded by a known constant, we first analyze the worst-case (upper and lower)

X. Zhang and Z. He are with the University of Electronic Science and Technology of China, Chengdu 611731, China (e-mail: xjzhang7@163.com; zshe@uestc.edu.cn).

X. P. Zhang is with Qian Xuesen Lab of Space Technology, Beijing 100094, China (e-mail: zhangxuepan@qxslab.cn).

boundaries of array response level. Then, given a sidelobe angle to be controlled, its upper response level, and an arbitrarily-specified weight vector, we follow the orthogonal decomposition model of C<sup>2</sup>-WORD in [1] and propose to accurately control the worst-case upper-boundary response level as desired. As presented later, the robust C<sup>2</sup>-WORD algorithm offers an analytical expression of weight vector updating and results less worst-case perturbation on the array response. In addition, inheriting the advantages of C<sup>2</sup>-WORD, our robust C<sup>2</sup>-WORD approach results small pattern variations on the uncontrolled points. To enhance the practicality of the devised algorithm, we also present how to determine the norm boundary of steering vector uncertainty, in the cases that array suffers from channel gain-phase mismatch, element position mismatch and mutual coupling effect, respectively. By applying the robust C<sup>2</sup>-WORD algorithm successively, we devise an effective robust sidelobe synthesis method. Simulations show that our algorithms work well under various circumstances.

This paper is organized as follows. The proposed robust C<sup>2</sup>-WORD algorithm is presented in Section II. In Section III, some practical considerations are provided to improve the practicality of robust C<sup>2</sup>-WORD. The application of robust C<sup>2</sup>-WORD to robust sidelobe synthesis is discussed in Section IV. Representative simulations are carried out in Section V and conclusions are drawn in Section VI.

*Notations:* Following the notations in [1], we use bold upper-case and lower-case letters to represent matrices and vectors, respectively. In particular, we use  $\mathbf{I}$  to denote the identity matrix.  $j \triangleq \sqrt{-1}$ .  $(\cdot)^T$  and  $(\cdot)^H$  stand for the transpose and Hermitian transpose, respectively.  $|\cdot|$  denotes the absolute value and  $\|\cdot\|_2$  denotes the  $l_2$  norm. We use  $\mathbf{B}(i, l)$  to stand for the element at the  $i$ th row and  $l$ th column of matrix  $\mathbf{B}$ .  $\mathbf{P}_{\mathbf{Z}}$  and  $\mathbf{P}_{\mathbf{Z}}^\perp$  represent the projection matrices onto  $\mathcal{R}(\mathbf{Z})$  and  $\mathcal{R}^\perp(\mathbf{Z})$ , respectively.  $\text{Diag}(\cdot)$  represents the diagonal matrix with the components of the input vector as the diagonal elements. Finally,  $\lambda_{\max}(\cdot)$  returns the largest eigenvalue of the input matrix.

## II. ROBUST SIDELOBE CONTROL VIA C<sup>2</sup>-WORD

### A. Robust Sidelobe Control Formulation

For the ease of later derivations, we first define the normalized magnitude response as

$$V_a(\theta) = |\mathbf{w}^H \mathbf{a}(\theta)| / |\mathbf{w}^H \mathbf{a}(\theta_0)| \quad (1)$$

where  $\mathbf{a}(\theta)$  denotes the nominal steering vector as defined in Eqn. (2) in [1],  $\theta_0$  stands for the main beam axis. Note that the above  $V_a(\theta)$  is different from the normalized power response  $L(\theta, \theta_0)$  defined in Eqn. (1) in [1]. One can readily find that  $V_a^2(\theta) = L(\theta, \theta_0)$ .

Clearly,  $V_a(\theta)$  describes the array magnitude response in the absence of array uncertainties. In practical, however, the steering vector is usually influenced by antenna array imperfections, such as, gain-phase mismatch, element position mismatch, mutual coupling effect and so on. In this case, the actual steering vector, denoted by  $\mathbf{b}(\theta)$ , is given by

$$\mathbf{b}(\theta) = \mathbf{a}(\theta) + \Delta(\theta) \quad (2)$$

where  $\Delta(\theta)$  is the unknown uncertainty that can be varied with  $\theta$ . The actual normalized magnitude response, denoted by  $V_b(\theta)$ , can be expressed as

$$V_b(\theta) = |\mathbf{w}^H \mathbf{b}(\theta)| / |\mathbf{w}^H \mathbf{b}(\theta_0)| \quad (3)$$

which is different from  $V_a(\theta)$  under normal circumstances. Note that in (3), we keep on using the output of  $\theta_0$  as the normalization factor, although the actual beam axis may have deviated slightly from  $\theta_0$  due to the steering vector uncertainties. In robust sidelobe control, we consider how to make the actual magnitude response  $V_b(\theta)$  lower than specific levels in certain sidelobe regions.

### B. Boundary Analysis on Array Response

To proceed, we first present a boundary analysis on the magnitude response  $V_b(\theta)$ . To do so, we reasonably suppose that the uncertainty  $\Delta(\theta)$  is norm-bounded as

$$\|\Delta(\theta)\|_2 \leq \varepsilon(\theta) \quad (4)$$

where  $\varepsilon(\theta)$  is a known constant at  $\theta$ . Then, according to the triangle inequality property, one gets

$$\begin{aligned} |\mathbf{w}^H \mathbf{b}(\theta)| &= |\mathbf{w}^H (\mathbf{a}(\theta) + \Delta(\theta))| \\ &\leq |\mathbf{w}^H \mathbf{a}(\theta)| + |\mathbf{w}^H \Delta(\theta)| \\ &\leq |\mathbf{w}^H \mathbf{a}(\theta)| + \|\mathbf{w}\|_2 \cdot \|\Delta(\theta)\|_2 \\ &\leq |\mathbf{w}^H \mathbf{a}(\theta)| + \varepsilon(\theta) \|\mathbf{w}\|_2. \end{aligned} \quad (5)$$

Similarly,

$$\begin{aligned} |\mathbf{w}^H \mathbf{b}(\theta)| &= |\mathbf{w}^H (\mathbf{a}(\theta) + \Delta(\theta))| \\ &\geq |\mathbf{w}^H \mathbf{a}(\theta)| - |\mathbf{w}^H \Delta(\theta)| \\ &\geq |\mathbf{w}^H \mathbf{a}(\theta)| - \|\mathbf{w}\|_2 \cdot \|\Delta(\theta)\|_2 \\ &\geq |\mathbf{w}^H \mathbf{a}(\theta)| - \varepsilon(\theta) \|\mathbf{w}\|_2. \end{aligned} \quad (6)$$

Combining (5) and (6), one can readily find that

$$\begin{aligned} V_b(\theta) &= \frac{|\mathbf{w}^H \mathbf{b}(\theta)|}{|\mathbf{w}^H \mathbf{b}(\theta_0)|} \\ &= \frac{|\mathbf{w}^H (\mathbf{a}(\theta) + \Delta(\theta))|}{|\mathbf{w}^H (\mathbf{a}(\theta_0) + \Delta(\theta_0))|} \\ &\leq \frac{|\mathbf{w}^H \mathbf{a}(\theta)| + \varepsilon(\theta) \|\mathbf{w}\|_2}{|\mathbf{w}^H \mathbf{a}(\theta_0)| - \varepsilon(\theta_0) \|\mathbf{w}\|_2} \\ &= \frac{V_a(\theta) + \varepsilon(\theta) \cdot \|\mathbf{w}\|_2 / |\mathbf{w}^H \mathbf{a}(\theta_0)|}{1 - \varepsilon(\theta_0) \cdot \|\mathbf{w}\|_2 / |\mathbf{w}^H \mathbf{a}(\theta_0)|} \\ &\triangleq V_u(\theta) \end{aligned} \quad (7)$$

and

$$\begin{aligned} V_b(\theta) &\geq \frac{|\mathbf{w}^H \mathbf{a}(\theta)| - \varepsilon(\theta) \|\mathbf{w}\|_2}{|\mathbf{w}^H \mathbf{a}(\theta_0)| + \varepsilon(\theta_0) \|\mathbf{w}\|_2} \\ &= \frac{V_a(\theta) - \varepsilon(\theta) \cdot \|\mathbf{w}\|_2 / |\mathbf{w}^H \mathbf{a}(\theta_0)|}{1 + \varepsilon(\theta_0) \cdot \|\mathbf{w}\|_2 / |\mathbf{w}^H \mathbf{a}(\theta_0)|} \\ &\triangleq V_l(\theta). \end{aligned} \quad (8)$$

Compactly, we have

$$0 \leq V_l(\theta) \leq V_b(\theta) \leq V_u(\theta) \quad (9)$$

where  $V_u(\theta)$  and  $V_l(\theta)$  stand for the worst-case upper and lower boundaries of magnitude response, respectively. According to (9), the actual response  $V_b(\theta)$  fluctuates in the range  $[V_l(\theta), V_u(\theta)]$ . In addition, it should be noted that we have implicitly assumed in (7) that

$$|\mathbf{w}^H \mathbf{a}(\theta_0)| - \varepsilon(\theta_0) \|\mathbf{w}\|_2 > 0. \quad (10)$$

Otherwise, it leads to  $V_u(\theta) < 0$  and (7) does not hold true.

### C. Robust One-Point Sidelobe Control Formulation

In the preceding subsection, a boundary analysis on the array response is presented. In this subsection, we formulate the problem of robust one-point sidelobe control, i.e., making the response level of a given sidelobe point lower than specific value in the presence of steering vector uncertainties.

More specifically, denote by  $V_d(\theta)$  the desired magnitude upper beam pattern. Give a previous weight vector  $\mathbf{w}_{k-1}$  and a sidelobe angle  $\theta_k$  to be controlled. It is required to find a new weight vector  $\mathbf{w}_k$  that makes the actual (magnitude) response level of  $\theta_k$  lower than  $V_d(\theta_k)$ . To simplify notations, in sequel we follow the usages of  $V_a(\theta)$ ,  $V_b(\theta)$ ,  $V_u(\theta)$  and  $V_l(\theta)$  defined in the two preceding subsections, and designate them to stand for the counterparts of  $\mathbf{w}_k$ . Then, the problem of one-point robust sidelobe control can be formulated as

$$\text{find } \mathbf{w}_k \quad (11a)$$

$$\text{subject to } V_b(\theta_k) \leq V_d(\theta_k). \quad (11b)$$

Note that there exists unknown perturbations on the steering vector, see (2). As a result, it may not be easy to adjust  $V_b(\theta_k)$  as desired.

To tackle problem (11), we recall (9) and formulate a conservative version of (11) as

$$\text{find } \mathbf{w}_k \quad (12a)$$

$$\text{subject to } V_u(\theta_k) \leq V_d(\theta_k) \quad (12b)$$

where the maximum possible response level at  $\theta_k$  (i.e.,  $V_u(\theta_k)$ ) is restricted to be lower than  $V_d(\theta_k)$ . Since  $V_b(\theta_k)$  is not greater than  $V_u(\theta_k)$ , one learns that the original constraint (11b) is satisfied if only (12b) holds true.

One possible way to make constraint (12b) qualified is to take  $V_u(\theta_k)$  as its minimum, which may be close to zero. By doing so, the actual response  $V_b(\theta_k)$  would also approach to zero because of the constraint (9). As a result, it may broaden the mainlobe of  $V_b(\theta)$  and/or lower the resulting WNG. To alleviate this drawback, a high value of  $V_b(\theta_k)$  is expected under the condition that (12b) is satisfied. As aforementioned,  $V_b(\theta_k)$  fluctuates in the range  $[V_l(\theta_k), V_u(\theta_k)]$ . Then, a reasonable way to elevate  $V_b(\theta_k)$  is to lift both the lower-boundary response level  $V_l(\theta_k)$  and the upper-boundary response level  $V_u(\theta_k)$ . According to (12b), the maximum of  $V_u(\theta_k)$  is  $V_d(\theta_k)$ , then we can improve the general level of  $V_b(\theta_k)$  by fixing  $V_u(\theta_k)$  as  $V_d(\theta_k)$  and then solving the following optimization problem:

$$\max_{\mathbf{w}_k} V_l(\theta_k) \quad (13a)$$

$$\text{subject to } V_u(\theta_k) = V_d(\theta_k). \quad (13b)$$

For the given  $V_a(\theta_k)$ ,  $\varepsilon(\theta_0)$  and  $\varepsilon(\theta_k)$ , it is not hard to observe from (7) and (8) that

$$V_u(\theta_k) - V_l(\theta_k) \propto \frac{\|\mathbf{w}_k\|_2}{|\mathbf{w}_k^H \mathbf{a}(\theta_0)|}. \quad (14)$$

Thus, one can reformulate problem (13) as:

$$\max_{\mathbf{w}_k} G(\mathbf{w}_k) \quad (15a)$$

$$\text{subject to } V_u(\theta_k) = V_d(\theta_k) \quad (15b)$$

where

$$G(\mathbf{w}) \triangleq \frac{|\mathbf{w}^H \mathbf{a}(\theta_0)|^2}{\|\mathbf{w}\|_2^2} \quad (16)$$

stands for the white noise gain (WNG) in the absence of steering vector uncertainties, and has also been defined in Eqn. (20) in [1]. As a matter of fact, since  $\|\mathbf{w}_k\|_2/|\mathbf{w}_k^H \mathbf{a}(\theta_0)|$  is directly proportional to the pattern perturbations, i.e.,  $V_u(\theta_k) - V_a(\theta_k)$  and  $V_a(\theta_k) - V_l(\theta_k)$ , the solution of problem (15) obtains small pattern perturbations for the given  $\varepsilon(\theta_0)$  and  $\varepsilon(\theta_k)$ .

Recalling the definition of  $V_u(\theta_k)$  in (7), we can reformulate the robust one-point sidelobe control problem (15) as

$$\max_{\mathbf{w}_k} G(\mathbf{w}_k) \quad (17a)$$

$$\text{subject to } V_a(\theta_k) = V_{\mathbf{w}}(\theta_k) \quad (17b)$$

where  $V_{\mathbf{w}}(\theta)$  is defined as

$$V_{\mathbf{w}}(\theta) \triangleq V_d(\theta) - \gamma(\theta) \|\mathbf{w}_k\|_2 / |\mathbf{w}_k^H \mathbf{a}(\theta_0)| \quad (18)$$

with  $\gamma(\theta) \triangleq V_d(\theta)\varepsilon(\theta_0) + \varepsilon(\theta)$ . Clearly, the non-convex problem (17) maximizes WNG with specific constraint on the (ideal) response level of  $\theta_k$ . This is similar to the response control problem formulated in Part I [1]. Nevertheless, different from the array response control problem discussed in [1], it should be noted that the right side of constraint (17b), i.e.,  $V_{\mathbf{w}}(\theta_k)$ , depends on the optimization variable  $\mathbf{w}_k$  as well. In addition, the previous weight vector  $\mathbf{w}_{k-1}$  is not taken into consideration in the formulating problem (17). As a result, it may lead to large pattern variations at the uncontrolled points, comparing to the previous beam pattern response. Recalling that the  $C^2$ -WORD scheme devised in Part I [1] maximizes WNG and results small pattern variations, this provides some inspiration to use  $C^2$ -WORD algorithm in [1] to realize one-point sidelobe control, as detailed in the next subsection.

### D. Robust $C^2$ -WORD Algorithm

In this subsection, we propose a new method to realize robust one-point sidelobe control and name it as robust  $C^2$ -WORD algorithm. The devised algorithm is built on the foundation of  $C^2$ -WORD scheme developed in [1] and can result small pattern variations at the uncontrolled points.

To begin with, we recall  $C^2$ -WORD scheme in [1], and incorporate a new constraint into (17) as

$$\max_{\beta_k} G(\mathbf{w}_k) \quad (19a)$$

$$\text{subject to } V_a(\theta_k) = V_{\mathbf{w}}(\theta_k) \quad (19b)$$

$$\mathbf{w}_k = [\mathbf{w}_{\perp} \quad \mathbf{w}_{\parallel}] [1 \quad \beta_k]^T, \beta_k \in \mathbb{C} \quad (19c)$$

where the constraint of orthogonal decomposition has been added in (19c), with  $\mathbf{w}_\perp$  and  $\mathbf{w}_\parallel$  satisfying

$$\mathbf{w}_\perp \triangleq \mathbf{P}_{[\mathbf{a}(\theta_k)]}^\perp \mathbf{w}_{k-1}, \quad \mathbf{w}_\parallel \triangleq \mathbf{P}_{[\mathbf{a}(\theta_k)]} \mathbf{w}_{k-1}. \quad (20)$$

Once the optimal  $\beta_{k,*}$  of (19) is obtained, we can express the ultimate weight vector  $\mathbf{w}_k$  as

$$\mathbf{w}_k = [\mathbf{w}_\perp \quad \mathbf{w}_\parallel] \begin{bmatrix} 1 & \beta_{k,*} \end{bmatrix}^T. \quad (21)$$

It should be emphasized that the resulting weight vector (21) may not be the global optimal solution of problem (17), since we have assigned a new constraint in problem (19). In spite of that, we will show later that the obtained  $\mathbf{w}_k$  in (21) performs well on robust sidelobe control with small pattern variations at the uncontrolled points. The remaining problem is how to determine the optimal  $\beta_{k,*}$  of (19), as presented next.

The  $C^2$ -WORD scheme in [1] is able to precisely control the array power response of a given point. For the sake of subsequent convenience, we first define

$$\rho_a \triangleq V_a^2(\theta_k) \quad (22)$$

which represents the ideal power response level at  $\theta_k$ . Then, for the given  $\theta_0$ ,  $\theta_k$ ,  $\mathbf{w}_{k-1}$ ,  $V_d(\theta_k)$ ,  $\varepsilon(\theta_0)$  and  $\varepsilon(\theta_k)$ , we can indirectly determine the optimal  $\beta_{k,*}$  by finding the corresponding  $\rho_a$  in problem (19).

After some calculation, one can see that the corresponding  $\rho_a$  of problem (19) satisfies the following quartic polynomial:

$$A^2 \rho_a^4 + (2AC - B^2) \rho_a^3 + (2AE - 2BD + C^2) \rho_a^2 + (2CE - D^2) \rho_a + E^2 = 0. \quad (23)$$

The derivation of (23) is presented in Appendix A, where the expressions of  $A, B, C, D, E$  are also specified, see (65). In fact, there are four candidates of  $\rho_a$  satisfying (23), and they can be analytically expressed, see the following Lemma to find their specific expressions.

*Lemma 1:* The four roots  $x_i$  ( $i = 1, 2, 3, 4$ ) for the following general quartic equation

$$ax^4 + bx^3 + cx^2 + dx + e = 0, \quad (a \neq 0) \quad (24)$$

are given by

$$x_1 = -\frac{b}{4a} + S + \frac{\sqrt{-4S^2 - 2p - \frac{q}{S}}}{2} \quad (25a)$$

$$x_2 = -\frac{b}{4a} + S - \frac{\sqrt{-4S^2 - 2p - \frac{q}{S}}}{2} \quad (25b)$$

$$x_3 = -\frac{b}{4a} - S + \frac{\sqrt{-4S^2 - 2p + \frac{q}{S}}}{2} \quad (25c)$$

$$x_4 = -\frac{b}{4a} - S - \frac{\sqrt{-4S^2 - 2p + \frac{q}{S}}}{2} \quad (25d)$$

where

$$p \triangleq \frac{8ac - 3b^2}{8a^2} \quad (26a)$$

$$q \triangleq \frac{b^3 - 4abc + 8a^2d}{8a^3} \quad (26b)$$

$$S \triangleq \frac{\sqrt{-\frac{2}{3}p + \frac{1}{3a} \left( Q + \frac{\zeta_0}{Q} \right)}}{2} \quad (26c)$$

---

### Algorithm 1 Robust $C^2$ -WORD Algorithm

---

- 1: prescribe beam axis  $\theta_0$  and index  $k$ , give the previous weight vector  $\mathbf{w}_{k-1}$ , sidelobe angle  $\theta_k$ , the desired (magnitude) upper response level  $V_d(\theta_k)$  and the steering vector uncertainty boundaries  $\varepsilon(\theta_0)$  and  $\varepsilon(\theta_k)$
  - 2: construct quartic equation (23) and find its solutions (i.e.,  $\rho_{a,1}, \rho_{a,2}, \rho_{a,3}, \rho_{a,4}$ ) from Lemma 1
  - 3: determine the ultimate  $\rho_{a,*}$  by solving problem (29)
  - 4: apply  $C^2$ -WORD algorithm to adjust the ideal array response of  $\theta_k$  to  $\rho_{a,*}$  and obtain the corresponding  $\beta_{k,*}$ , see Algorithm 1 in [1]
  - 5: output the new weight vector  $\mathbf{w}_k$  in (21)
- 

with

$$Q \triangleq \sqrt[3]{\left( \zeta_1 + \sqrt{\zeta_1^2 - 4\zeta_0^3} \right) / 2} \quad (27a)$$

$$\zeta_0 \triangleq c^2 - 3bd + 12ae \quad (27b)$$

$$\zeta_1 \triangleq 2c^3 - 9bcd + 27b^2e + 27ad^2 - 72ace. \quad (27c)$$

*Proof:* See [15]. ■

According to (25) in Lemma 1, we can similarly obtain the four solutions of quartic equation (23), and denote them as  $\rho_{a,1}, \rho_{a,2}, \rho_{a,3}, \rho_{a,4}$ , respectively. Recalling our previous discussions, we note that the qualified  $\rho_a$  is real-valued and satisfies

$$\rho_a \in [0, V_d^2(\theta_k)]. \quad (28)$$

Then, to obtain the maximal  $V_a(\theta_k)$ , we can obtain the final  $\rho_{a,*}$  by solving the following simple problem:

$$\max_{\rho_a} \rho_a \quad (29a)$$

$$\text{subject to } \rho_a \in \{\rho_{a,1}, \rho_{a,2}, \rho_{a,3}, \rho_{a,4}\} \quad (29b)$$

$$\rho_a \in [0, V_d^2(\theta_k)]. \quad (29c)$$

Once the optimal  $\rho_{a,*}$  is determined, we can remove the constraint (19b) and reformulate problem (19) as

$$\max_{\beta_k} G(\mathbf{w}_k) \quad (30a)$$

$$\text{subject to } L_k(\theta_k, \theta_0) = \rho_{a,*} \quad (30b)$$

$$\mathbf{w}_k = [\mathbf{w}_\perp \quad \mathbf{w}_\parallel] \begin{bmatrix} 1 & \beta_k \end{bmatrix}^T, \quad \beta_k \in \mathbb{C} \quad (30c)$$

where  $L_k(\theta, \theta_0) = |\mathbf{w}_k^H \mathbf{a}(\theta)|^2 / |\mathbf{w}_k^H \mathbf{a}(\theta_0)|^2$ . The above problem (30) has an analytical solution, see Proposition 2 in Part I [1] for details. Thus, we can obtain the ultimate  $\beta_{k,*}$  and its corresponding weight vector  $\mathbf{w}_k$  in (21). This completes the robust one-point response control at a given sidelobe point. Finally, we summarize the proposed robust  $C^2$ -WORD algorithm in Algorithm 1.

#### E. Restriction Between $V_d(\theta_k)$ and $\varepsilon(\theta_k)$

In the preceding subsection, we use the  $C^2$ -WORD scheme to realize robust sidelobe control at a pre-assigned angle  $\theta_k$ . It should be pointed out that there exists an implicit restriction between the minimum reachable upper response level  $V_d(\theta_k)$

and the steering vector uncertainty norm boundary  $\varepsilon(\theta_k)$ , as investigated next.

To begin with, we note that  $V_a(\theta_k) \geq 0$ . Since  $V_a(\theta_k)$  is generally in proportional to  $V_u(\theta_k)$ , we can obtain the minimum reachable level of  $V_d(\theta_k)$  (denoted as  $\bar{V}_d(\theta_k)$ ) by setting  $V_a(\theta_k) = 0$ . Recalling (18) and (19b),  $\bar{V}_d(\theta_k)$  is given by

$$\begin{aligned}\bar{V}_d(\theta_k) &= \gamma(\theta_k) \|\mathbf{w}_k\|_2 / |\mathbf{w}_k^H \mathbf{a}(\theta_0)| \\ &= (\bar{V}_d(\theta_k) \varepsilon(\theta_0) + \varepsilon(\theta_k)) \cdot \|\mathbf{w}_k\|_2 / |\mathbf{w}_k^H \mathbf{a}(\theta_0)| \\ &= (\bar{V}_d(\theta_k) \varepsilon(\theta_0) + \varepsilon(\theta_k)) \cdot \|\mathbf{w}_\perp\|_2 / |\mathbf{w}_\perp^H \mathbf{a}(\theta_0)|\end{aligned}\quad (31)$$

where we have utilized the fact that  $\beta_\star = 0$  and  $\mathbf{w}_k = \mathbf{w}_\perp$  when  $V_a(\theta_k) = 0$  applies. According to (31),  $V_d(\theta_k)$  should be taken to satisfy:

$$V_d(\theta_k) \geq \bar{V}_d(\theta_k) = \frac{\varepsilon(\theta_k) \|\mathbf{w}_\perp\|_2}{|\mathbf{w}_\perp^H \mathbf{a}(\theta_0)| - \varepsilon(\theta_0) \|\mathbf{w}_\perp\|_2} \quad (32)$$

which specifies the restriction between  $V_d(\theta_k)$  and  $\varepsilon(\theta_k)$  for the given  $\varepsilon(\theta_0)$  and  $\mathbf{a}(\theta_0)$ . Clearly, the less  $\varepsilon(\theta_k)$  is, the lower level  $V_d(\theta_k)$  can be taken.

Note from (32) that the minimum reachable level of  $V_d(\theta_k)$  (i.e.,  $\bar{V}_d(\theta_k)$ ) depends on the previous weight vector  $\mathbf{w}_{k-1}$  as well. Utilizing the Cauchy-Schwarz inequality that  $\|\mathbf{w}_\perp\|_2 \|\mathbf{a}(\theta_0)\|_2 \geq |\mathbf{w}_\perp^H \mathbf{a}(\theta_0)|$ , one can further obtain:

$$V_d(\theta_k) \geq \bar{V}_d(\theta_k) \geq \frac{\varepsilon(\theta_k)}{\|\mathbf{a}(\theta_0)\|_2 - \varepsilon(\theta_0)} \triangleq \chi(\theta_k) \quad (33)$$

where the introduced  $\chi(\theta_k)$  is independent of the weight vector and specifies a lower boundary of  $\bar{V}_d(\theta_k)$ . Note that the resulting  $\chi(\theta_k)$  in (33) gives a general value of the minimum achievable level of  $V_d(\theta_k)$ , although it may not be reached for an arbitrarily-specified previous weight  $\mathbf{w}_{k-1}$ .

### III. PRACTICAL CONSIDERATION

In the preceding section, a robust  $C^2$ -WORD algorithm is devised to adjust the response level of a pre-assigned sidelobe point with steering vector perturbation. As aforementioned, the steering vector uncertainty  $\Delta(\theta)$  is assumed to be norm-bounded by a known constant  $\varepsilon(\theta)$ . To enhance the practicality of robust  $C^2$ -WORD algorithm, we next consider how to determine  $\Delta(\theta)$  and the corresponding  $\varepsilon(\theta)$  in practical applications with some reasonable assumptions.

In this paper, we assume that the array suffers from channel gain-phase mismatch, element position mismatch, mutual coupling effect or their superpositions. On this basis, we can model the actual steering vector  $\mathbf{b}(\theta)$  in (2) as

$$\mathbf{b}(\theta) = \mathbf{C}(\theta) \mathbf{a}(\theta) = \mathbf{a}(\theta) + \underbrace{[\mathbf{C}(\theta) - \mathbf{I}] \mathbf{a}(\theta)}_{\Delta(\theta)} \quad (34)$$

where  $\mathbf{C}(\theta)$  is a certain matrix whose elements may vary with  $\theta$ . Let us define

$$\mathbf{E}(\theta) \triangleq \mathbf{C}(\theta) - \mathbf{I}. \quad (35)$$

Then according to (34), we have  $\Delta(\theta) = \mathbf{E}(\theta) \mathbf{a}(\theta)$ , from which one can further derive that

$$\|\Delta(\theta)\|_2 = \|\mathbf{E}(\theta) \mathbf{a}(\theta)\|_2 \leq \|\mathbf{E}(\theta)\|_2 \|\mathbf{a}(\theta)\|_2 \quad (36)$$

where  $\|\mathbf{E}(\theta)\|_2$  is the spectral matrix norm [16] of  $\mathbf{E}(\theta)$  satisfying

$$\|\mathbf{E}(\theta)\|_2 = \sqrt{\lambda_{\max}(\mathbf{E}^H(\theta) \mathbf{E}(\theta))}. \quad (37)$$

Clearly, if  $\mathbf{E}(\theta)$  is known or can be estimated, we can set the corresponding  $\varepsilon(\theta)$  in (4) as

$$\varepsilon(\theta) = \|\mathbf{E}(\theta)\|_2 \|\mathbf{a}(\theta)\|_2. \quad (38)$$

However, this is not a common occurrence, since  $\mathbf{E}(\theta)$  (or  $\mathbf{C}(\theta)$ ) is usually a random matrix with certain statistical model for its entries [17]. In this case, we can determine  $\varepsilon(\theta)$  by

$$\varepsilon(\theta) = \|\mathbf{a}(\theta)\|_2 \cdot \max \|\mathbf{E}(\theta)\|_2. \quad (39)$$

We next present some specific scenarios, in which the steering vector uncertainty boundary  $\varepsilon(\theta)$  can be analytically expressed according to (39). For the sake of simplicity, we only consider linear arrays, although the extension to more complicated configurations are straightforward.

#### A. Channel Gain-phase Mismatch

To begin with, we consider the channel gain-phase mismatch [18]–[20]. In this case, we have

$$\mathbf{C}(\theta) = \text{Diag}([1, g_2 e^{j\varphi_2}, \dots, g_N e^{j\varphi_N}]) \quad (40)$$

where  $g_n$  and  $\varphi_n$  stand for the channel gain and phase errors of the  $n$ th element, respectively,  $n = 2, \dots, N$ . Note that the measurements have been normalized by that of the first element. Accordingly,  $\mathbf{E}(\theta)$  can be expressed as

$$\mathbf{E}(\theta) = \text{Diag}([0, g_2 e^{j\varphi_2} - 1, \dots, g_N e^{j\varphi_N} - 1]). \quad (41)$$

Recalling (37), we have

$$\max \|\mathbf{E}(\theta)\|_2 = \max_{n=2, \dots, N} |g_n e^{j\varphi_n} - 1|. \quad (42)$$

Suppose that  $g_n$  and  $\varphi_n$  are randomly distributed in certain regions as

$$g_n \in [g_{n,l}, g_{n,u}], \quad \varphi_n \in [\varphi_{n,l}, \varphi_{n,u}], \quad n = 2, \dots, N \quad (43)$$

where  $g_l$ ,  $g_u$ ,  $\varphi_l$  and  $\varphi_u$  are corresponding boundaries. On this basis, we can obtain from (42) that

$$\max \|\mathbf{E}(\theta)\|_2 = \max_{n \in \{2, \dots, N\}, \tau \in \{l, u\}, \varsigma \in \{l, u\}} |g_{n,\tau} e^{j\varphi_{n,\varsigma}} - 1| \triangleq \delta_1.$$

According to (39), one can set  $\varepsilon(\theta)$  as

$$\varepsilon(\theta) = \|\mathbf{a}(\theta)\|_2 \cdot \delta_1. \quad (44)$$

#### B. Element Position Mismatch

We next analyze the steering vector uncertainty  $\Delta(\theta)$  and determine its corresponding  $\varepsilon(\theta)$  when array elements suffer from position uncertainties [21]. In this case,  $\mathbf{C}(\theta)$  is given by

$$\mathbf{C}(\theta) = \text{Diag}([1, e^{j2\pi\alpha_2 \sin(\theta)/\lambda}, \dots, e^{j2\pi\alpha_N \sin(\theta)/\lambda}]) \quad (45)$$

where  $\lambda$  stands for wavelength,  $\alpha_n$  represents the position deviation of the  $n$ th element from its ideal location  $d_n$ ,  $n = 2, \dots, N$ . According to (35), one can express  $\mathbf{E}(\theta)$  as

$$\mathbf{E}(\theta) = \text{Diag}([0, e^{j2\pi\alpha_2 \sin(\theta)/\lambda} - 1, \dots, e^{j2\pi\alpha_N \sin(\theta)/\lambda} - 1]).$$

Suppose that  $\alpha_n$  is randomly distributed in the range as

$$\alpha_n \in [\alpha_{n,l}, \alpha_{n,u}], \quad n = 2, \dots, N \quad (46)$$

where  $\alpha_{n,l}$  and  $\alpha_{n,u}$  are known boundaries. Then, we can obtain the following result about  $\mathbf{E}(\theta)$ , i.e.,

$$\max \|\mathbf{E}(\theta)\|_2 = \max_{n \in \{2, \dots, N\}, \tau \in \{l, u\}} |e^{j2\pi\alpha_{n,\tau}\sin(\theta)/\lambda} - 1| \triangleq \delta_2(\theta).$$

Different from the  $\delta_1$  in Section III.A, the above  $\delta_2(\theta)$  is directionally dependent. Finally, according to (39), we can set  $\varepsilon(\theta)$  as

$$\varepsilon(\theta) = \|\mathbf{a}(\theta)\|_2 \cdot \delta_2(\theta). \quad (47)$$

### C. Mutual Coupling Effect

Now we consider the steering vector uncertainty arising from mutual coupling effect [22]–[24]. Following [17], we only consider the electromagnetic coupling between nonadjacent elements of a linear array, and express the mutual coupling matrix  $\mathbf{C}(\theta)$  as

$$\mathbf{C}(\theta) = \begin{bmatrix} 1 & \xi \cdot z_{1,2} & 0 & \cdots & 0 \\ \xi \cdot z_{2,1} & 1 & \xi \cdot z_{2,3} & \ddots & \vdots \\ 0 & \xi \cdot z_{3,2} & 1 & \ddots & 0 \\ \vdots & \ddots & \ddots & 1 & \xi \cdot z_{N-1,N} \\ 0 & \cdots & 0 & \xi \cdot z_{N,N-1} & 1 \end{bmatrix}$$

which is complex symmetry. In  $\mathbf{C}(\theta)$ ,  $\xi$  is the known isolation between channels,  $z_{i,j}$  are random variables with a fixed magnitude  $|z_{i,j}| = 1$ . Recalling (35), we have

$$\mathbf{E}(\theta) = \xi \cdot \begin{bmatrix} 0 & z_{1,2} & 0 & \cdots & 0 \\ z_{2,1} & 0 & z_{2,3} & \ddots & \vdots \\ 0 & z_{3,2} & 0 & \ddots & 0 \\ \vdots & \ddots & \ddots & 0 & z_{N-1,N} \\ 0 & \cdots & 0 & z_{N,N-1} & 0 \end{bmatrix}. \quad (48)$$

According to the Gershgorin circle theorem [25], i.e.,

$$|\lambda_{\max}(\mathbf{D})| \leq \max_{p=1, \dots, P} \sum_{l=1}^L |\mathbf{D}(p, l)| \quad (49)$$

where  $\mathbf{D}$  is a  $P \times L$  matrix, it can be concluded that

$$\max \|\mathbf{E}(\theta)\|_2 = \sqrt{\lambda_{\max}(\mathbf{E}^H(\theta)\mathbf{E}(\theta))} \leq 2\xi \triangleq \delta_3. \quad (50)$$

From (39), we can set  $\varepsilon(\theta)$  as

$$\varepsilon(\theta) = \|\mathbf{a}(\theta)\|_2 \cdot \delta_3 = 2\xi \|\mathbf{a}(\theta)\|_2. \quad (51)$$

## IV. ROBUST SIDELOBE SYNTHESIS

In this section, we introduce the application of robust  $\text{C}^2$ -WORD algorithm to sidelobe synthesis with steering vector imperfections. The general strategy is similar to the concept of pattern synthesis using  $\text{C}^2$ -WORD in Part I [1]. However, different from the pattern synthesis approach in [1], we realize robust sidelobe synthesis by successively adjusting the worst-case upper-boundary magnitude pattern (i.e.,  $V_u(\theta)$ ), but not the ideal beam pattern  $V_a(\theta)$ . For the sake of clarity, in sequel

## Algorithm 2 Proposed Robust Sidelobe Synthesis Algorithm

- 1: give  $\theta_0, \varepsilon(\theta)$ , the desired magnitude upper pattern  $V_d(\theta)$ , the initial weight vector  $\mathbf{w}_0$  and its corresponding worst-case upper-boundary pattern  $V_{u,0}(\theta)$ , set  $k = 1$
- 2: **while** 1 **do**
- 3:   select an angle  $\theta_k$  by comparing  $V_{u,k-1}(\theta)$  with  $V_d(\theta)$
- 4:   apply robust  $\text{C}^2$ -WORD to realize  $V_{u,k}(\theta_k) = V_d(\theta_k)$ , obtain  $\mathbf{w}_k$  in (21) and the corresponding  $V_{u,k}(\theta)$
- 5:   **if**  $V_{u,k}(\theta)$  is not satisfactory **then**
- 6:     set  $k = k + 1$
- 7:   **else**
- 8:     **break**
- 9:   **end if**
- 10: **end while**
- 11: output  $\mathbf{w}_k$

TABLE I  
ELEMENT POSITIONS OF THE NON-UNIFORM LINEAR ARRAY

$n$	$x_n(\lambda)$	$n$	$x_n(\lambda)$	$n$	$x_n(\lambda)$	$n$	$x_n(\lambda)$
1	0.00	4	1.55	7	3.05	10	4.55
2	0.45	5	2.10	8	3.65	11	5.05
3	1.00	6	2.60	9	4.10	12	5.50

we incorporate the subscript  $k$  into  $V_a(\theta)$  and  $V_u(\theta)$ , and use  $V_{a,k}(\theta)$  and  $V_{u,k}(\theta)$  to stand for the counterparts of  $\mathbf{w}_k$ .

More precisely, an initial ideal pattern  $V_{a,0}(\theta)$  and the corresponding worst-case upper-boundary pattern  $V_{u,0}(\theta)$  are firstly obtained from (1) and (7), respectively, by setting the initial weight vector as  $\mathbf{w}_0$ . Then, following the angle selection strategy in Part I [1], we choose an angle  $\theta_1$ , at which  $V_{u,0}(\theta)$  has peak point and produces a higher level than the desired upper pattern  $V_d(\theta)$ . Next, the robust  $\text{C}^2$ -WORD scheme is applied to modify the weight vector  $\mathbf{w}_0$  to  $\mathbf{w}_1$ , by setting the output of  $V_{u,1}(\theta_1)$  as  $V_d(\theta_1)$ . Similarly, by comparing  $V_{u,1}(\theta)$  with  $V_d(\theta)$ , a second angle  $\theta_2$ , at which the response is needed to be adjusted, is selected. An updated weight vector  $\mathbf{w}_2$  can thus be achieved via robust  $\text{C}^2$ -WORD. The above procedure is carried out successively once the sidelobe responses of  $V_{u,k}(\theta)$  are lower than  $V_d(\theta)$ . To make the above descriptions clear, we summarize the proposed robust sidelobe synthesis algorithm in Algorithm 2.

## V. NUMERICAL RESULTS

We next present some simulations to show the effectiveness of the proposed robust  $\text{C}^2$ -WORD scheme on array response control and pattern synthesis under various settings. To see the superiority of our algorithm, the results of WORD algorithm in [26] and convex programming (CP) method in [2] are also presented if applicable. Unless otherwise specified, we take  $\mathbf{a}(\theta_0)$  as the initial weight for both WORD and robust  $\text{C}^2$ -WORD.

### A. Illustration of Robust Sidelobe Control

In this part, we illustrate the performance of robust  $\text{C}^2$ -WORD on sidelobe control at a given point. In the first

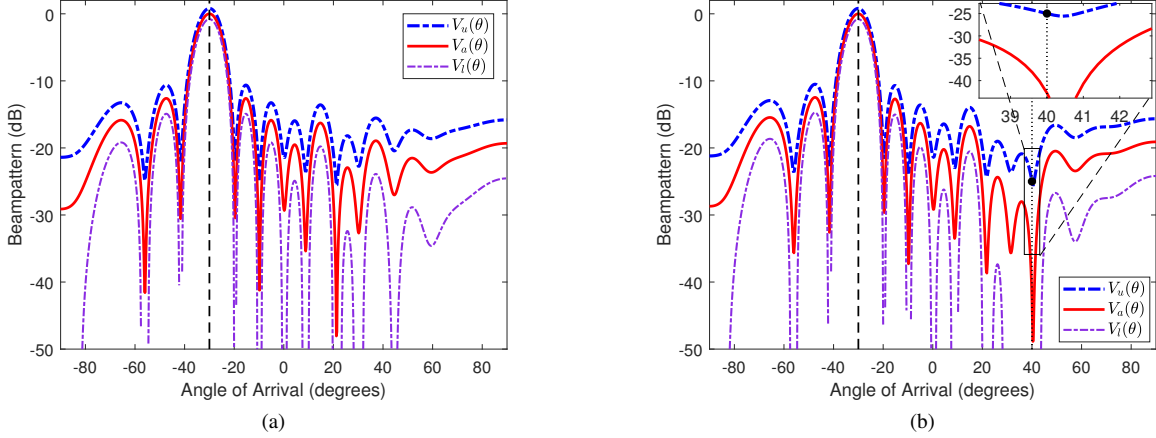


Fig. 1. Illustration of response control for a non-uniformly spaced linear array. (a) Before array response control. (b) After array response control.

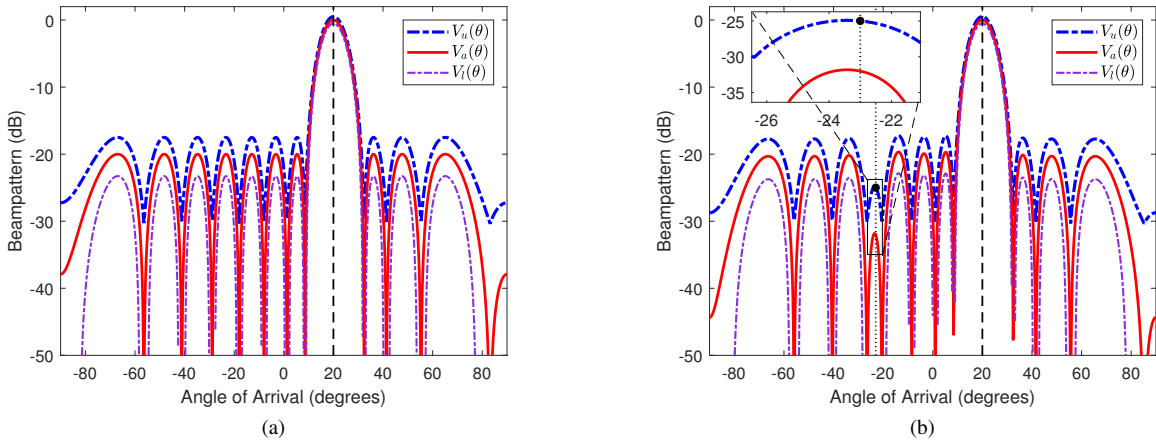


Fig. 2. Illustration of response control for a uniformly spaced linear array. (a) Before array response control. (b) After array response control.

example, we consider a non-uniformly spaced linear array with 12 elements, see Table I for its element positions. The beam axis is steered to  $\theta_0 = -30^\circ$  and the norm boundary of steering vector is taken as  $\varepsilon(\theta) = 0.16$ . In this case, it is required to adjust the (actual) sidelobe response at  $\theta_1 = 40^\circ$  to be lower than  $V_d(\theta_1) = -25\text{dB}$ . Fig. 1(a) depicts the ideal beampattern  $V_a(\theta)$  of the initial weight vector  $\mathbf{w}_0 = \mathbf{a}(\theta_0)$ , the corresponding worst-case upper-boundary pattern  $V_u(\theta)$  and the lower-boundary pattern  $V_l(\theta)$ .

Applying our robust  $C^2$ -WORD algorithm and after some calculation, we can figure out that  $\rho_{a,*} = -42.7746\text{dB}$ ,  $\beta_{1,*} = 0.077$ . Fig. 1(b) presents the resulting beampatterns of the weight vector  $\mathbf{w}_1$ . It is shown that the upper-boundary response level at  $\theta_1$  (i.e.,  $V_u(\theta_1)$ ) has been precisely adjusted to be  $V_d(\theta_1) = -25\text{dB}$ . Since  $V_u(\theta)$  is the worst-case upper boundary of the sidelobe response, we know that all the actual response level at  $\theta_1$  is lower than  $u_1$ , if only  $\|\Delta(\theta)\|_2 \leq \varepsilon(\theta)$  is satisfied. In addition, comparing to the beampatterns in Fig. 1(a), it should be noted that the resulting beampatterns in Fig. 1(b) are almost unchanged at the uncontrolled points (i.e.,  $\theta \neq \theta_1$ ). This benefit comes essentially from the advantage of  $C^2$ -WORD algorithm developed in Part I [1].

To further show that our algorithm is effective for an

arbitrarily-specified initial weight, we consider a 12-element uniformly spaced linear array (ULA) and steer its beam axis to  $\theta_0 = 20^\circ$ . In this case, we take the initial weight of robust  $C^2$ -WORD as the Chebyshev weight with a  $-20\text{dB}$  sidelobe attenuation. The norm boundary of steering vector uncertainties is taken as  $\varepsilon(\theta) = 0.1$ . It is required to adjust the (actual) response level at  $\theta_1 = -23^\circ$  to be lower than  $V_d(\theta_1) = -25\text{dB}$ . Fig. 2(a) shows the corresponding  $V_a(\theta)$ ,  $V_u(\theta)$  and  $V_l(\theta)$  of the initial weight. After carrying out the proposed robust  $C^2$ -WORD scheme, we obtain that  $\rho_{a,*} = -31.9987\text{dB}$  and  $\beta_{1,*} = 0.2506$ . The resulting beampatterns are presented in Fig. 2(b), from which we find that the value of  $V_u(\theta_1)$  equals exactly to  $V_d(\theta_1) = -25\text{dB}$ . Also, it can be checked from Fig. 2 that our algorithm results small pattern variations at the unadjusted points after the robust response control step. In addition, we note that the resulting  $\beta_{1,*}$ 's are real-valued in the above two testings. In fact, these are two special cases that have been discussed in Part I [1]. A complex-valued  $\beta_*$  will be resulted in general circumstances.

### B. Robust Sidelobe Synthesis Using Robust $C^2$ -WORD

In this section, representative simulations are presented to illustrate the application of robust  $C^2$ -WORD to sidelobe

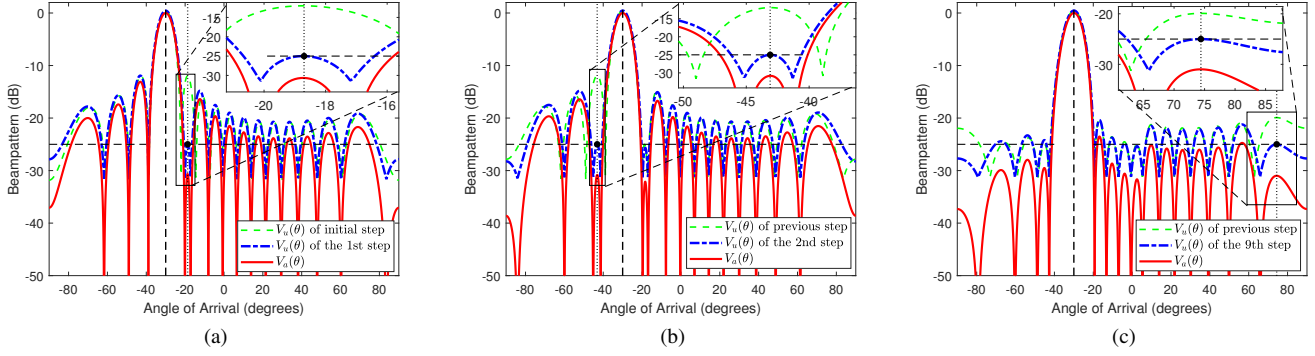


Fig. 3. Synthesis procedure of uniform-sidelobe pattern using a ULA. (a) Synthesized pattern at the first step. (b) Synthesized pattern at the second step. (c) Synthesized pattern at the 9th step.

TABLE II  
OBTAINED WEIGHTINGS OF ROBUST  $C^2$ -WORD WHEN SYNTHESIZING  
UNIFORM SIDELOBE PATTERN FOR A ULA

$n$	$w_n$	$n$	$w_n$	$n$	$w_n$
1	$0.34e^{-j0.80}$	7	$1.25e^{+j2.35}$	13	$0.77e^{-j0.78}$
2	$0.39e^{-j2.37}$	8	$1.31e^{+j0.78}$	14	$0.58e^{-j2.35}$
3	$0.58e^{+j2.35}$	9	$1.31e^{-j0.78}$	15	$0.39e^{+j2.37}$
4	$0.77e^{+j0.78}$	10	$1.25e^{-j2.35}$	16	$0.34e^{+j0.80}$
5	$0.96e^{-j0.79}$	11	$1.13e^{+j2.36}$		
6	$1.13e^{-j2.36}$	12	$0.96e^{+j0.79}$		

synthesis with steering vector uncertainties.

1) *Uniform Sidelobe Synthesis for a ULA*: In the first example, a 16-element ULA is considered. We steer the beam axis to  $\theta_0 = -30^\circ$ . The desired upper beampattern has  $-25$ dB uniform sidelobe level and the steering vector uncertainty  $\Delta(\theta)$  is assumed to be norm-bounded by  $\varepsilon(\theta) = 0.1$ .

Fig. 3 presents several intermediate results when synthesizing pattern with robust  $C^2$ -WORD algorithm. In the first step, our algorithm compares the worst-case upper-boundary pattern  $V_{u,0}(\theta)$  of the initial weight with the desired pattern  $V_d(\theta)$ . Then, we choose  $\theta_1 = -18.7^\circ$  according to our angle selection strategy described in Section IV. Applying robust  $C^2$ -WORD, we figure out that  $\rho_{a,*} = -30.6544$ dB and  $\beta_{1,*} = 0.1276$  in the first step. The resulting beampatterns are depicted in Fig. 3(a), from which we can see that the upper-boundary response level  $V_{u,1}(\theta_1)$  has been precisely adjusted as its desired level (i.e.,  $-25$ dB). Based on the resulting  $\mathbf{w}_1$  and  $V_{u,1}(\theta)$ , we conduct the second step of robust  $C^2$ -WORD algorithm and figure out that  $\theta_2 = -43.1^\circ$ ,  $\rho_{a,*} = -30.8132$ dB and  $\beta_{1,*} = 0.1245$ . The obtained beampatterns are illustrated in Fig. 3(b), from which we can check that  $V_{u,2}(\theta_2) = -25$ dB. After applying the robust  $C^2$ -WORD algorithm iteratively, the envelope of  $V_u(\theta)$  becomes closer to  $V_d(\theta)$ , and we can terminate the iteration if a satisfactory  $V_u(\theta)$  has been synthesized.

Following [1], we define  $D_k$  to explore the convergence of the proposed approach. More specifically,  $D_k$  measures the the maximum response deviation within the set of sidelobe peak angles at the  $k$ th step (denoted by  $\Omega_s^k$ ) and is given by

$$D_k \triangleq \max_{\theta \in \Omega_s^k} (V_{u,k}(\theta) - V_d(\theta)). \quad (52)$$

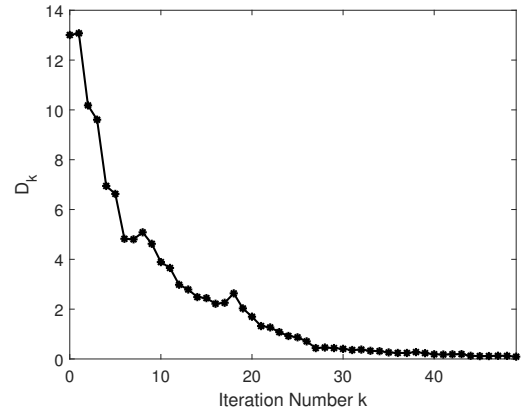


Fig. 4. Maximum response deviation  $D_k$  versus the iteration number.

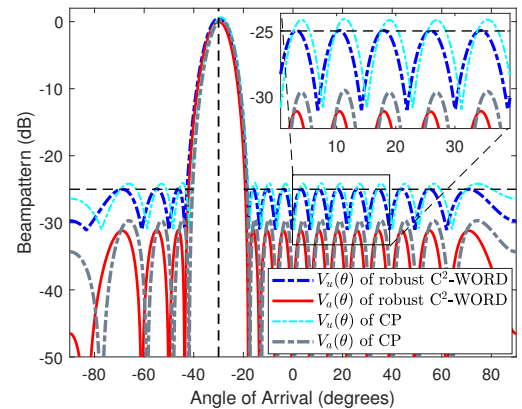


Fig. 5. Synthesized patterns with uniform sidelobe for a ULA.

The curve of  $D_k$  versus the iterative number  $k$  is depicted in Fig. 4, which clearly shows that  $D_k$  decreases with the increase of iteration. After carrying out 50 response control steps, the resulting  $D_k$  equals approximately to zero and we terminate the synthesis process. Table II presents the resulting weight vector of our algorithm. Interestingly, it is found that the weights are centro-symmetric. A possible explanation is that the array utilized has a symmetry structure.

The ultimate beampatterns are depicted in Fig. 5. We can



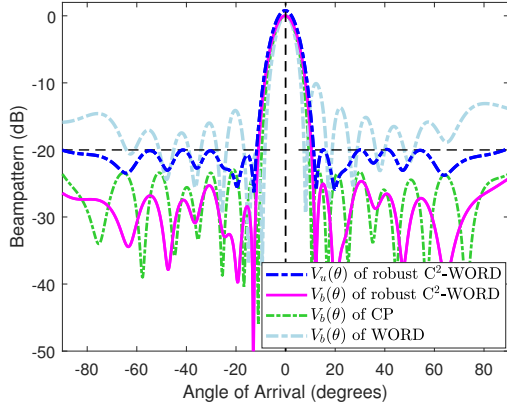


Fig. 6. Synthesized patterns for a circular arc array with gain-phase mismatch.

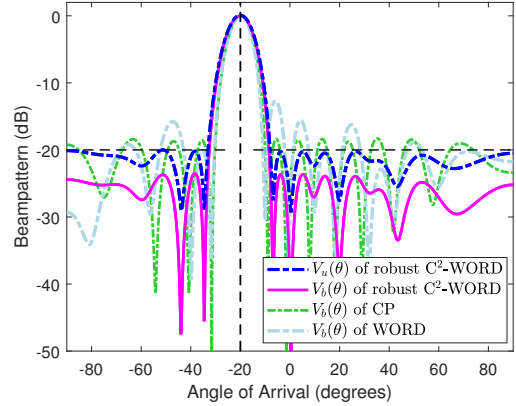


Fig. 7. Synthesized patterns for a linear array with element position mismatch.

TABLE III  
OBTAINED WEIGHTINGS OF ROBUST C<sup>2</sup>-WORD WITH CHANNEL  
PHASE-GAIN MISMATCH

$n$	$w_n$	$n$	$w_n$	$n$	$w_n$
1	$0.27e^{-j1.56}$	7	$1.26e^{+j3.10}$	13	$0.49e^{-j0.69}$
2	$0.37e^{+j1.42}$	8	$1.37e^{-j2.69}$	14	$0.44e^{-j2.21}$
3	$0.43e^{-j2.16}$	9	$1.35e^{-j2.71}$	15	$0.34e^{+j1.36}$
4	$0.50e^{-j0.60}$	10	$1.25e^{+j3.06}$	16	$0.26e^{-j1.67}$
5	$0.91e^{+j0.97}$	11	$1.07e^{+j2.26}$		
6	$1.08e^{+j2.31}$	12	$0.91e^{+j0.93}$		

see that the resulting worst-case upper-boundary pattern  $V_u(\theta)$  of our algorithm aligns with the desired sidelobe level. For the CP method in [2], we set the mainlobe region as  $[-42^\circ, -18^\circ]$  and obtain an upper-boundary pattern  $V_u(\theta)$  with a uniform sidelobe level, as shown in Fig. 5. For CP approach, the resulting maximum sidelobe level of  $V_u(\theta)$  is about  $-24$ dB, which is higher than that of the proposed robust C<sup>2</sup>-WORD algorithm. In fact, there is a trade-off between the mainlobe width and the sidelobe level for CP method. Moreover, it's not clear how to determine the mainlobe width of CP approach for a given sidelobe level requirement.

2) *Uniform Sidelobe Synthesis With Channel Phase-Gain Mismatch*: In this example, we consider a circular arc array with 16 nonisotropic elements, see Fig. 9 in [1] with  $\theta_c = 60^\circ$ . The beam axis is taken as  $\theta_0 = 0^\circ$  and the sidelobe level is expected to be lower than  $-20$ dB. The distance between adjacent elements is half a wavelength and there exists channel phase-gain uncertainties on sensor elements. More specifically, the phase error  $\varphi_n$  and gain error  $g_n$  are uniformly distributed in  $[-0.035, 0.035]$  and  $[0.98, 1.02]$ , respectively,  $n = 2, \dots, N$ . Following the analysis in Section III.A, we can figure out  $\delta_1 = 0.039$  and then obtain the upper norm boundary  $\varepsilon(\theta)$  according to (44).

Fig. 6 presents the resulting worst-case upper-boundary pattern  $V_u(\theta)$  of robust C<sup>2</sup>-WORD algorithm after 20 iteration steps, and Table III lists the obtained weight vector. It can be clearly observed that the sidelobe envelope of  $V_u(\theta)$  is aligned with the desired upper pattern  $V_d(\theta)$ . To compare the performances of different approaches, Fig. 6 also demonstrates the realizations of actual beampattern  $V_b(\theta)$ . We can see that

TABLE IV  
OBTAINED WEIGHTINGS OF ROBUST C<sup>2</sup>-WORD WITH ELEMENT  
POSITION MISMATCH

$n$	$w_n$	$n$	$w_n$	$n$	$w_n$
1	$0.32e^{-j0.16}$	5	$1.08e^{+j1.78}$	9	$0.77e^{-j2.60}$
2	$0.67e^{-j0.89}$	6	$1.17e^{+j0.77}$	10	$0.64e^{+j2.73}$
3	$0.75e^{-j2.17}$	7	$1.07e^{-j0.40}$	11	$0.48e^{+j1.80}$
4	$1.04e^{+j2.90}$	8	$1.08e^{-j1.47}$	12	$0.34e^{+j0.62}$

the actual beampatterns of robust C<sup>2</sup>-WORD and CP satisfy the pre-assigned response requirement, while the WORD algorithm does not.

3) *Uniform Sidelobe Synthesis With Element Position Mismatch*: We now carry out robust uniform sidelobe synthesis by considering array element position mismatch. More specifically, we use a 12-element non-uniformly spaced linear array, see Table I for its (ideal) element positions. The beam axis is steered to  $\theta_0 = -20^\circ$  and the upper level of the desired sidelobe response is  $-20$ dB. The array suffers from element position perturbation and the location deviation is uniformly distributed in  $[-0.5\% \lambda, 0.5\% \lambda]$ . Under these settings, we can determine  $\varepsilon(\theta)$  according to (47) and realize robust sidelobe synthesis using our robust C<sup>2</sup>-WORD algorithm.

Fig. 7 presents the resulting  $V_u(\theta)$  of robust C<sup>2</sup>-WORD algorithm after 50 iteration steps, and Table IV gives the obtained weight vector. As expected, the obtained upper-boundary beampattern  $V_u(\theta)$  satisfies the pre-assigned response requirement. To show the superiority of our algorithm, we also depict the realizations of real beampattern  $V_b(\theta)$  for different methods. Fig. 7 shows that the real beampatterns of CP and WORD result unqualified responses on sidelobe region. For the robust C<sup>2</sup>-WORD algorithm, the obtained  $V_b(\theta)$  meets our requirement with a sidelobe level about  $-25$ dB.

4) *Nonuniform Sidelobe Synthesis With Mutual Coupling Effect*: In this example, we consider a 20-element ULA and set the beam axis as  $\theta_0 = -30^\circ$ . Following the mutual coupling model in Section III.C, we take mutual coupling effect into consideration by setting the channel isolation as  $\xi = -35$ dB. With these configurations, one can readily determine the upper boundary  $\varepsilon(\theta)$  from (51). Different from the previous testings,

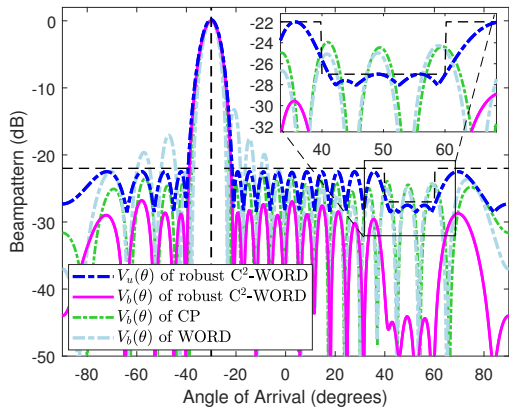


Fig. 8. Synthesized patterns for a ULA with mutual coupling effect.

TABLE V  
OBTAINED WEIGHTINGS OF ROBUST C<sup>2</sup>-WORD WITH MUTUAL COUPLING EFFECT

$n$	$w_n$	$n$	$w_n$	$n$	$w_n$
1	$0.40e^{-j0.07}$	8	$1.16e^{+j1.58}$	15	$0.95e^{+j3.14}$
2	$0.46e^{-j1.37}$	9	$1.28e^{+j0.01}$	16	$0.84e^{+j1.55}$
3	$0.54e^{+j3.01}$	10	$1.28e^{-j1.59}$	17	$0.63e^{-j0.06}$
4	$0.63e^{+j1.64}$	11	$1.28e^{-j3.12}$	18	$0.54e^{-j1.44}$
5	$0.84e^{+j0.02}$	12	$1.28e^{+j1.56}$	19	$0.46e^{+j2.94}$
6	$0.95e^{-j1.57}$	13	$1.16e^{-j0.01}$	20	$0.40e^{+j1.65}$
7	$1.08e^{-j3.14}$	14	$1.08e^{-j1.57}$		

in this case we consider a non-uniform desired upper sidelobe  $V_d(\theta)$ . More specifically, the upper level is  $-22$ dB in the region  $[40^\circ, 60^\circ]$  and  $-27$ dB in the rest of the sidelobe region.

Fig. 8 shows the resulting  $V_u(\theta)$  of the proposed robust C<sup>2</sup>-WORD algorithm after 80 iteration steps, and Table V lists the corresponding weight vector. Though the desired sidelobe level is non-uniform, we can see clearly that  $V_u(\theta)$  satisfies the pre-assigned requirement. Fig. 8 also depicts the realizations of real beampattern (i.e.,  $V_b(\theta)$ ) for robust C<sup>2</sup>-WORD, CP and WORD. It is observed that the robust C<sup>2</sup>-WORD algorithm obtains a qualified beampattern  $V_b(\theta)$  with non-uniform sidelobe shape. The resulting sidelobe of CP method is uniform and does not satisfy the pre-assigned requirement in the null region. As for WORD, the maximal sidelobe level of  $V_b(\theta)$  is about  $-13$ dB, which is also an undesirable result.

## VI. CONCLUSIONS

In this paper, we have presented a new algorithm named robust C<sup>2</sup>-WORD, which can realize robust sidelobe control and synthesis with steering vector mismatch. The proposed robust C<sup>2</sup>-WORD algorithm offers an analytical expression of weight vector updating and is able to precisely control the worst-case upper-boundary response level of a given sidelobe point for the norm-bounded steering vector uncertainties. We have also presented detailed analyses on how to determine the norm boundary of steering vector uncertainty under various mismatch circumstances. Moreover, a robust sidelobe synthesis approach has been devised by successively applying robust

C<sup>2</sup>-WORD algorithm. The applications of robust C<sup>2</sup>-WORD to robust sidelobe control and synthesis have been validated with various examples. As a future work, we shall consider the robust multi-point response control algorithm so as to reduce the number of iteration step in synthesis process.

## APPENDIX A DERIVATION OF (23)

To simplify the notation, we omit the subscript of  $\beta$  in sequel. According to the definition of  $\rho_a$  in (22), we have

$$\sqrt{\rho_a} = |\mathbf{w}_k^H \mathbf{a}(\theta_k)| / |\mathbf{w}_k^H \mathbf{a}(\theta_0)|. \quad (53)$$

Recalling the constraint (19b), we can expand it as

$$\sqrt{\rho_a} = V_d(\theta_k) - \frac{\gamma(\theta_k) \|\mathbf{w}_k\|_2}{|\mathbf{w}_k^H \mathbf{a}(\theta_0)|} \quad (54)$$

$$= V_d(\theta_k) - \frac{\sqrt{\rho_a} \gamma(\theta_k) \|\mathbf{w}_k\|_2}{|\mathbf{w}_k^H \mathbf{a}(\theta_k)|} \quad (55)$$

where Eqn. (53) has been utilized. Substituting the constraint (19c) into  $\mathbf{w}_k$ , one obtains

$$\frac{|\mathbf{w}_k^H \mathbf{a}(\theta_k)|^2}{\|\mathbf{w}_k\|_2^2} = \frac{|\beta|^2 |\mathbf{w}_\parallel^H \mathbf{a}(\theta_k)|^2}{\|\mathbf{w}_\perp\|_2^2 + |\beta|^2 \|\mathbf{w}_\parallel\|_2^2}. \quad (56)$$

Then, we can reformulate Eqn. (54) as

$$V_d(\theta_k) - \sqrt{\rho_a} = \frac{\sqrt{\rho_a} \gamma(\theta_k)}{\sqrt{\frac{|\beta|^2 |\mathbf{w}_\parallel^H \mathbf{a}(\theta_k)|^2}{\|\mathbf{w}_\perp\|_2^2 + |\beta|^2 \|\mathbf{w}_\parallel\|_2^2}}} \quad (57)$$

or equivalently,

$$|\beta|^2 = \frac{\left( \frac{\sqrt{\rho_a} \gamma(\theta_k)}{V_d(\theta_k) - \sqrt{\rho_a}} \right)^2 \|\mathbf{w}_\perp\|_2^2}{|\mathbf{w}_\parallel^H \mathbf{a}(\theta_k)|^2 - \left( \frac{\sqrt{\rho_a} \gamma(\theta_k)}{V_d(\theta_k) - \sqrt{\rho_a}} \right)^2 \|\mathbf{w}_\parallel\|_2^2}. \quad (58)$$

On the other hand, recalling from Proposition 2 in Part I [1] that  $\beta$  satisfies

$$|\beta| = |\mathbf{c}_\beta| + R_\beta \quad (59)$$

with

$$|\mathbf{c}_\beta| = \frac{\rho_a |\mathbf{w}_\perp^H \mathbf{a}(\theta_0)| \cdot |\mathbf{w}_\parallel^H \mathbf{a}(\theta_0)|}{|\mathbf{B}(2, 2)|} \quad (60)$$

$$R_\beta = \frac{\sqrt{\rho_a} |\mathbf{w}_\perp^H \mathbf{a}(\theta_0)| \cdot |\mathbf{w}_\parallel^H \mathbf{a}(\theta_k)|}{|\mathbf{B}(2, 2)|} \quad (61)$$

where  $\mathbf{B}$  is given by

$$\mathbf{B} = \begin{bmatrix} \mathbf{w}_\parallel^H \mathbf{a}(\theta_k) \\ \mathbf{w}_\parallel^H \mathbf{a}(\theta_k) \end{bmatrix} \begin{bmatrix} \mathbf{w}_\parallel^H \mathbf{a}(\theta_k) \\ \mathbf{w}_\parallel^H \mathbf{a}(\theta_k) \end{bmatrix}^H - \rho_a \begin{bmatrix} \mathbf{w}_\perp^H \mathbf{a}(\theta_0) \\ \mathbf{w}_\perp^H \mathbf{a}(\theta_0) \end{bmatrix} \begin{bmatrix} \mathbf{w}_\perp^H \mathbf{a}(\theta_0) \\ \mathbf{w}_\perp^H \mathbf{a}(\theta_0) \end{bmatrix}^H. \quad (62)$$

Thus, we have

$$|\beta| = \frac{\rho_a |\mathbf{w}_\perp^H \mathbf{a}(\theta_0)| \cdot |\mathbf{w}_\parallel^H \mathbf{a}(\theta_0)| + \sqrt{\rho_a} |\mathbf{w}_\perp^H \mathbf{a}(\theta_0)| \cdot |\mathbf{w}_\parallel^H \mathbf{a}(\theta_k)|}{\left| \frac{\rho_a |\mathbf{w}_\perp^H \mathbf{a}(\theta_0)| \cdot |\mathbf{w}_\parallel^H \mathbf{a}(\theta_0)|}{|\mathbf{w}_\parallel^H \mathbf{a}(\theta_k)|^2 - \rho_a |\mathbf{w}_\parallel^H \mathbf{a}(\theta_0)|^2} \right|}.$$

Substituting the above  $|\beta|$  into (58), we can eliminate  $\beta$  and obtain a quartic equation with respect to  $\rho_a$  as shown in (63)

$$\left( \frac{\rho_a |\mathbf{w}_\perp^H \mathbf{a}(\theta_0)| \cdot |\mathbf{w}_\parallel^H \mathbf{a}(\theta_0)| + \sqrt{\rho_a} |\mathbf{w}_\perp^H \mathbf{a}(\theta_0)| \cdot |\mathbf{w}_\parallel^H \mathbf{a}(\theta_k)|}{|\mathbf{w}_\parallel^H \mathbf{a}(\theta_k)|^2 - \rho_a |\mathbf{w}_\parallel^H \mathbf{a}(\theta_0)|^2} \right)^2 = \frac{\left( \frac{\sqrt{\rho_a} \gamma(\theta_k)}{V_d(\theta_k) - \sqrt{\rho_a}} \right)^2 \|\mathbf{w}_\perp\|_2^2}{|\mathbf{w}_\parallel^H \mathbf{a}(\theta_k)|^2 - \left( \frac{\sqrt{\rho_a} \gamma(\theta_k)}{V_d(\theta_k) - \sqrt{\rho_a}} \right)^2 \|\mathbf{w}_\parallel\|_2^2} \quad (63)$$

$$A = (|\mathbf{w}_\parallel^H \mathbf{a}(\theta_k)|^2 - \gamma^2(\theta_k) \|\mathbf{w}_\parallel\|_2^2) \cdot |\mathbf{w}_\perp^H \mathbf{a}(\theta_0)|^2 \cdot |\mathbf{w}_\parallel^H \mathbf{a}(\theta_0)|^2 - \gamma^2(\theta_k) \|\mathbf{w}_\perp\|_2^2 \cdot |\mathbf{w}_\parallel^H \mathbf{a}(\theta_0)|^4 \quad (65a)$$

$$B = 2 \left( (|\mathbf{w}_\parallel^H \mathbf{a}(\theta_k)|^2 - \gamma^2(\theta_k) \|\mathbf{w}_\parallel\|_2^2) - V_d(\theta_k) \cdot |\mathbf{w}_\parallel^H \mathbf{a}(\theta_0)| |\mathbf{w}_\parallel^H \mathbf{a}(\theta_k)| \right) |\mathbf{w}_\perp^H \mathbf{a}(\theta_0)|^2 \cdot |\mathbf{w}_\parallel^H \mathbf{a}(\theta_0)| \cdot |\mathbf{w}_\parallel^H \mathbf{a}(\theta_k)| \quad (65b)$$

$$C = V_d^2(\theta_k) |\mathbf{w}_\parallel^H \mathbf{a}(\theta_k)|^2 \cdot |\mathbf{w}_\perp^H \mathbf{a}(\theta_0)|^2 \cdot |\mathbf{w}_\parallel^H \mathbf{a}(\theta_0)|^2 + (|\mathbf{w}_\parallel^H \mathbf{a}(\theta_k)|^2 - \gamma^2(\theta_k) \|\mathbf{w}_\parallel\|_2^2) \cdot |\mathbf{w}_\parallel^H \mathbf{a}(\theta_k)|^2 \cdot |\mathbf{w}_\perp^H \mathbf{a}(\theta_0)|^2 - 4V_d(\theta_k) |\mathbf{w}_\parallel^H \mathbf{a}(\theta_k)|^3 \cdot |\mathbf{w}_\perp^H \mathbf{a}(\theta_0)| \cdot |\mathbf{w}_\parallel^H \mathbf{a}(\theta_0)|^2 + 2\gamma^2(\theta_k) \|\mathbf{w}_\perp\|_2^2 \cdot |\mathbf{w}_\parallel^H \mathbf{a}(\theta_k)|^2 \cdot |\mathbf{w}_\parallel^H \mathbf{a}(\theta_0)|^2 \quad (65c)$$

$$D = 2V_d(\theta_k) |\mathbf{w}_\parallel^H \mathbf{a}(\theta_k)|^3 \cdot |\mathbf{w}_\perp^H \mathbf{a}(\theta_0)|^2 \cdot (V_d(\theta_k) |\mathbf{w}_\parallel^H \mathbf{a}(\theta_0)| - |\mathbf{w}_\parallel^H \mathbf{a}(\theta_k)|) \quad (65d)$$

$$E = |\mathbf{w}_\parallel^H \mathbf{a}(\theta_k)|^4 \cdot (V_d^2(\theta_k) |\mathbf{w}_\perp^H \mathbf{a}(\theta_0)|^2 - \gamma^2(\theta_k) \cdot \|\mathbf{w}_\perp\|_2^2) \quad (65e)$$

on the top of this page. After some manipulations, one can reshape (63) as

$$A\rho_k^2 + B\rho_a\sqrt{\rho_a} + C\rho_a + D\sqrt{\rho_a} + E = 0 \quad (64)$$

where the coefficients  $A$ ,  $B$ ,  $C$ ,  $D$  and  $E$  are given in (65) on the top of this page. Eqn. (64) can be alternatively expressed as

$$A\rho_k^2 + C\rho_a + E = -\sqrt{\rho_a}(B\rho_a + D). \quad (66)$$

Taking square to both sides of (66) yields

$$A^2\rho_a^4 + (2AC - B^2)\rho_a^3 + (2AE - 2BD + C^2)\rho_a^2 + (2CE - D^2)\rho_a + E^2 = 0. \quad (67)$$

This completes the derivation of (23).

## REFERENCES

- [1] X. Zhang, Z. He, and X. Zhang, "Pattern synthesis via complex-coefficient weight vector orthogonal decomposition—Part I: Fundamentals," preprint, Aug. 2018.
- [2] S. Yan and J. M. Hovem, "Array pattern synthesis with robustness against manifold vectors uncertainty," *IEEE J. Ocean. Eng.*, vol. 33, pp. 405-413, 2008.
- [3] T. Zhang and W. Ser, "Robust beam pattern synthesis for antenna arrays with mutual coupling effect," *IEEE Trans. Antennas Propag.*, vol. 59, pp. 2889-2895, 2011.
- [4] M. S. Hossain, G. N. Milford, M. C. Reed, and L. C. Godara, "Robust efficient broadband antenna array pattern synthesis techniques," *IEEE Trans. Antennas Propag.*, vol. 62, pp. 4537-4546, 2014.
- [5] S. A. Vorobyov, A. B. Gershman, and Z. Q. Luo, "Robust adaptive beamforming using worst-case performance optimization: a solution to the signal mismatch problem," *IEEE Trans. Signal Process.*, vol. 51, pp. 313-324, 2003.
- [6] B. Liao, K. M. Tsui, and S. C. Chan, "Robust beamforming with magnitude response constraints using iterative second-order cone programming," *IEEE Trans. Antennas Propag.*, vol. 59, pp. 3477-3482, 2011.
- [7] S. E. Nai, W. Ser, Z. L. Yu, and S. Rahardja, "A robust adaptive beamforming framework with beam pattern shaping constraints," *IEEE Trans. Antennas Propag.*, vol. 57, pp. 2198-2203, 2009.
- [8] Z. L. Yu, M. H. Er, and W. Ser, "A novel adaptive beamformer based on semidefinite programming (SDP) with magnitude response constraints," *IEEE Trans. Antennas Propag.*, vol. 56, pp. 1297-1307, 2008.
- [9] D. D. Feldman and L. J. Griffiths, "A projection approach for robust adaptive beamforming," *IEEE Trans. Signal Process.*, vol. 42, pp. 867-876, 1994.
- [10] L. Tenuti, N. Anselmi, P. Rocca, M. Salucci, and A. Massa, "Minkowski sum method for planar arrays sensitivity analysis with uncertain-but-bounded excitation tolerances," *IEEE Trans. Antennas Propag.*, vol. 65, pp. 167-177, 2017.
- [11] N. Anselmi, L. Manica, P. Rocca, and A. Massa, "Tolerance analysis of antenna arrays through interval arithmetic," *IEEE Trans. Antennas Propag.*, vol. 61, pp. 5496-5507, 2013.
- [12] P. Rocca, N. Anselmi, and A. Massa, "Optimal synthesis of robust beamformer weights exploiting interval analysis and convex optimization," *IEEE Trans. Antennas Propag.*, vol. 62, pp. 3603-3612, 2014.
- [13] L. Poli, P. Rocca, N. Anselmi, and A. Massa, "Dealing with uncertainties on phase weighting of linear antenna arrays by means of interval-based tolerance analysis," *IEEE Trans. Antennas Propag.*, vol. 63, pp. 3229-3234, 2015.
- [14] N. Hu, B. Duan, W. Xu, and J. Zhou, "A new interval pattern analysis method of array antennas based on Taylor expansion," *IEEE Trans. Antennas Propag.*, vol. 65, pp. 6151-6156, 2017.
- [15] S. L. Shmakov, "A universal method of solving quartic equations," *International Journal of Pure and Applied Mathematics*, vol. 71, pp. 251-259, 2011.
- [16] G. H. Golub and C. F. V. Loan, *Matrix Computations*. Baltimore, MD: The Johns Hopkins Univ. Press, 1996.
- [17] C. M. Schmid, S. Schuster, R. Feger, and A. Stelzer, "On the effects of calibration errors and mutual coupling on the beam pattern of an antenna array," *IEEE Trans. Antennas Propag.*, vol. 61, pp. 4063-4072, 2013.
- [18] B. Liao and S. C. Chan, "Direction finding with partly calibrated uniform linear arrays," *IEEE Trans. Antennas Propag.*, vol. 60, pp. 922-929, 2012.
- [19] N. Boon Chong and S. Chong Meng Samson, "Sensor-array calibration using a maximum-likelihood approach," *IEEE Trans. Antennas Propag.*, vol. 44, pp. 827-835, 1996.
- [20] Z. Ming and Z. Zhaoda, "A method for direction finding under sensor gain and phase uncertainties," *IEEE Trans. Antennas Propag.*, vol. 43, pp. 880-883, 1995.
- [21] K. C. Ho and L. Yang, "On the use of a calibration emitter for source localization in the presence of sensor position uncertainty," *IEEE Trans. Signal Process.*, vol. 56, pp. 5758-5772, 2008.
- [22] B. Friedlander and A. J. Weiss, "Direction finding in the presence of mutual coupling," *IEEE Trans. Antennas Propag.*, vol. 39, pp. 273-284, 1991.
- [23] D. F. Kelley and W. L. Stutzman, "Array antenna pattern modeling methods that include mutual coupling effects," *IEEE Trans. Antennas Propag.*, vol. 41, pp. 1625-1632, 1993.
- [24] Q. Yuan, Q. Chen, and K. Sawaya, "Performance of adaptive array antenna with arbitrary geometry in the presence of mutual coupling," *IEEE Trans. Antennas Propag.*, vol. 54, pp. 1991-1996, 2006.
- [25] J. W. Demmel, *Applied Numerical Linear Algebra*. Philadelphia, PA, USA: SIAM, 1997.
- [26] X. Zhang, Z. He, B. Liao, X. Zhang, and W. Peng, "Pattern synthesis for arbitrary arrays via weight vector orthogonal decomposition," *IEEE Trans. Signal Process.*, vol. 66, pp. 1286-1299, 2018.